Phase diagram of rotating QCD with $N_f = 2$ clover-improved Wilson fermions

A. A. Roenko,

in collaboration with

V. V. Braguta, A. Yu. Kotov, D. A. Sychev

Joint Institute for Nuclear Research, Bogoliubov Laboratory of Theoretical Physics

roenko@theor.jinr.ru

The XXVI International Scientific Conference of Young Scientists and Specialists (AYSS-2022),
Dubna, 24-28 October 2022

Introduction

- In non-central heavy ion collisions creation of QGP with angular momentum is expected.

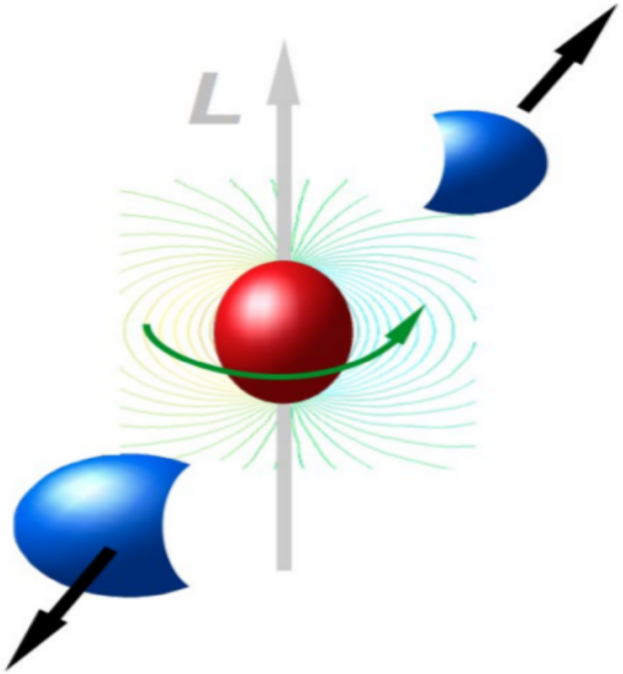

Introduction

- In non-central heavy ion collisions creation of QGP with angular momentum is expected.
- The rotation occurs with relativistic velocities.

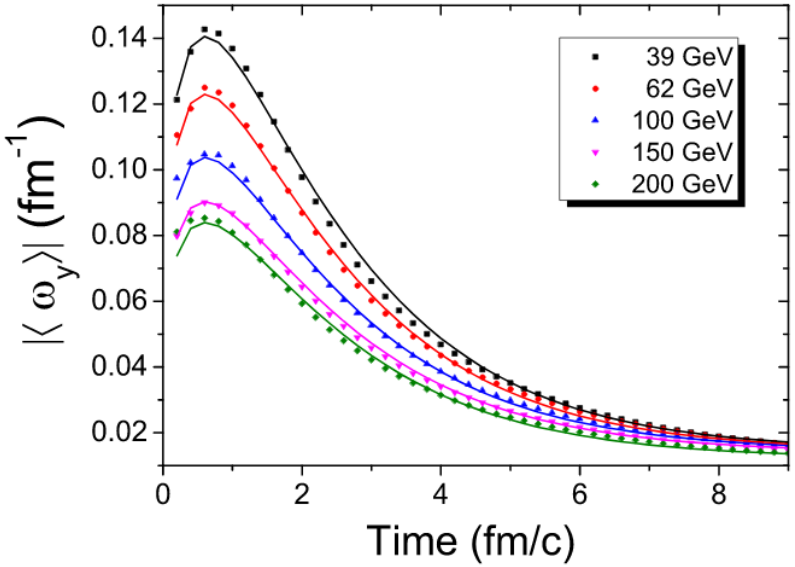

Au+Au, $b = 7$ fm

[Y. Jiang et al., Phys. Rev. C **94**, 044910 (2016), arXiv:1602.06580 [hep-ph]]

$\omega \sim 0.1 - 0.2\,\mathrm{fm}^{-1} \sim 20 - 40$ MeV

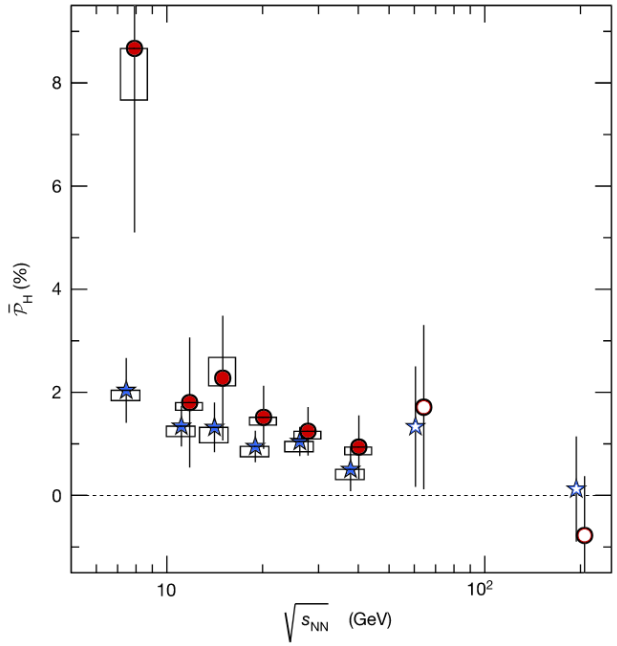

[L. Adamczyk et al. (STAR), Nature **548**, 62–65 (2017), arXiv:1701.06657 [nucl-ex]]

$\omega \sim 6$ MeV ($\sqrt{s_{NN}}$-averaged)

Introduction

- In non-central heavy ion collisions creation of QGP with angular momentum is expected.
- The rotation occurs with relativistic velocities.

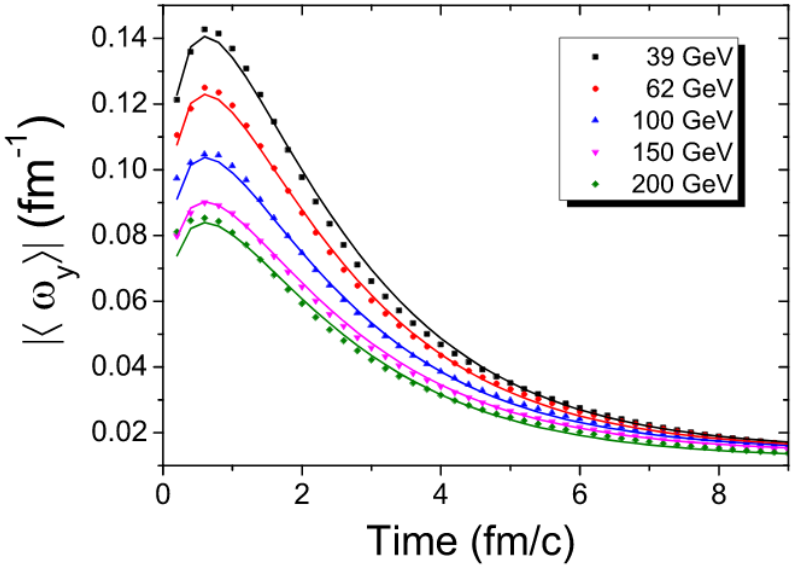

Au+Au, $b = 7$ fm

[Y. Jiang et al., Phys. Rev. C **94**, 044910 (2016), arXiv:1602.06580 [hep-ph]]

$\omega \sim 0.1 - 0.2\,\mathrm{fm}^{-1} \sim 20 - 40$ MeV

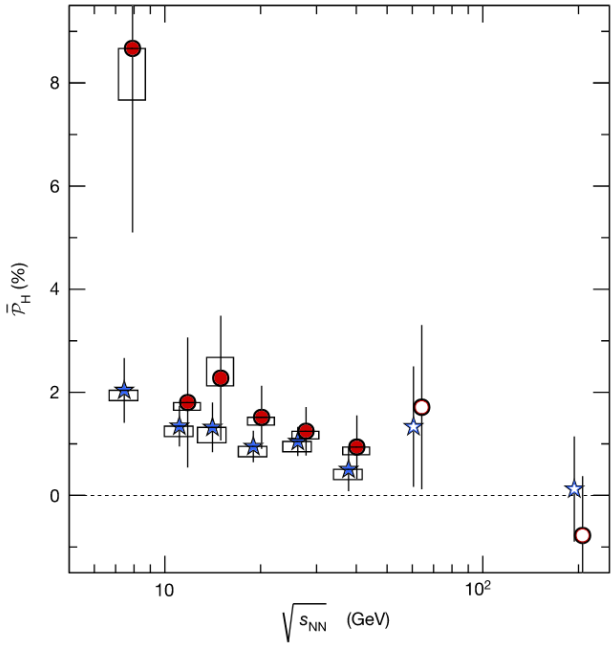

[L. Adamczyk et al. (STAR), Nature **548**, 62–65 (2017), arXiv:1701.06657 [nucl-ex]]

$\omega \sim 6$ MeV ($\sqrt{s_{NN}}$-averaged)

- How does the rotation affect to phase transitions in QCD?

Related papers

NJL (and other phenomenological models) predicts that critical temperature decreases due to the rotation.

Related papers

NJL (and other phenomenological models) predicts that critical temperature decreases due to the rotation.

The rotation affects both gluon and quark degrees of freedom!

Related papers

NJL (and other phenomenological models) predicts that critical temperature decreases due to the rotation.

The rotation affects both gluon and quark degrees of freedom!

Our lattice results for gluodynamics is opposite: critical temperature increases with rotation.

- V. V. Braguta et al., JETP Lett. **112**, 6–12 (2020)
- V. V. Braguta et al., Phys. Rev. D **103**, 094515 (2021), arXiv:2102.05084 [hep-lat]
- V. Braguta et al., PoS **LATTICE2021**, 125 (2022), arXiv:2110.12302 [hep-lat]

Related papers

NJL (and other phenomenological models) predicts that critical temperature decreases due to the rotation.

The rotation affects both gluon and quark degrees of freedom!

Our lattice results for gluodynamics is opposite: critical temperature increases with rotation.

- V. V. Braguta et al., JETP Lett. **112**, 6–12 (2020)
- V. V. Braguta et al., Phys. Rev. D **103**, 094515 (2021), arXiv:2102.05084 [hep-lat]
- V. Braguta et al., PoS **LATTICE2021**, 125 (2022), arXiv:2110.12302 [hep-lat]

Taking into account the contribution of rotating gluons to NJL model:

- Y. Jiang, (2021), arXiv:2108.09622 [hep-ph]

Related papers

NJL (and other phenomenological models) predicts that critical temperature decreases due to the rotation.

The rotation affects both gluon and quark degrees of freedom!

Our lattice results for gluodynamics is opposite: critical temperature increases with rotation.

- V. V. Braguta et al., JETP Lett. **112**, 6–12 (2020)
- V. V. Braguta et al., Phys. Rev. D **103**, 094515 (2021), arXiv:2102.05084 [hep-lat]
- V. Braguta et al., PoS **LATTICE2021**, 125 (2022), arXiv:2110.12302 [hep-lat]

Taking into account the contribution of rotating gluons to NJL model:

- Y. Jiang, (2021), arXiv:2108.09622 [hep-ph]

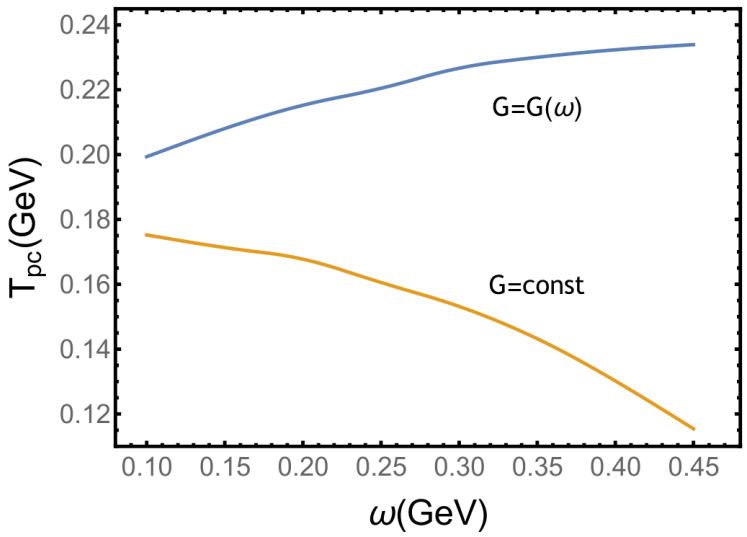

The running effective coupling $G(\omega)$ is introduced.

$\Rightarrow$ Critical temperature increases due to the rotation.

Rotating reference frame

- QCD (at thermal equilibrium) is investigated in the reference frame which rotates with the system with angular velocity Ω .
- In this reference frame there appears an external gravitational field

$$g_{\mu\nu} = \begin{pmatrix} 1 - r^2\Omega^2 & \Omega y & -\Omega x & 0 \\ \Omega y & -1 & 0 & 0 \\ -\Omega x & 0 & -1 & 0 \\ 0 & 0 & 0 & -1 \end{pmatrix} .$$

[1] A. Yamamoto and Y. Hirono, Phys. Rev. Lett. **111**, 081601 (2013), arXiv:1303.6292 [hep-lat].

Rotating reference frame

- QCD (at thermal equilibrium) is investigated in the reference frame which rotates with the system with angular velocity Ω .
- In this reference frame there appears an external gravitational field

$$g_{\mu\nu} = \begin{pmatrix} 1 - r^2\Omega^2 & \Omega y & -\Omega x & 0 \\ \Omega y & -1 & 0 & 0 \\ -\Omega x & 0 & -1 & 0 \\ 0 & 0 & 0 & -1 \end{pmatrix} .$$

[1] A. Yamamoto and Y. Hirono, Phys. Rev. Lett. **111**, 081601 (2013), arXiv:1303.6292 [hep-lat].

Rotating reference frame

- QCD (at thermal equilibrium) is investigated in the reference frame which rotates with the system with angular velocity Ω .
- In this reference frame there appears an external gravitational field

$$g_{\mu\nu} = \begin{pmatrix} 1 - r^2\Omega^2 & \Omega y & -\Omega x & 0 \\ \Omega y & -1 & 0 & 0 \\ -\Omega x & 0 & -1 & 0 \\ 0 & 0 & 0 & -1 \end{pmatrix} .$$

- The partition function is[1]

$$Z = \int D\psi \, D\bar{\psi} \, DA \, \exp\big(- S_G[A, \Omega] - S_F[\bar{\psi}, \psi, A, m, \Omega] \big) . \tag{1}$$

[1] A. Yamamoto and Y. Hirono, Phys. Rev. Lett. **111**, 081601 (2013), arXiv:1303.6292 [hep-lat].

Rotating QCD: continuum action

The Euclidean gluon action can be written as

$$S_G = \frac{1}{4g^2} \int d^4x \sqrt{g_E}\, g_E^{\mu\nu} g_E^{\alpha\beta} F^a_{\mu\alpha} F^a_{\nu\beta} \,. \tag{2}$$

And the quark action reads as follows[2]

$$S_F = \int d^4x \sqrt{g_E}\, \bar{\psi}\big(\gamma^\mu (D_\mu - \Gamma_\mu) + m\big)\psi \,, \tag{3}$$

The covariant derivative D_μ and spinor affine connection Γ_μ is

$$D_\mu = \partial_\mu - iA_\mu \,, \tag{4}$$

$$\Gamma_\mu = -\frac{i}{4}\sigma^{ij}\omega_{\mu ij} \,, \tag{5}$$

$$\sigma^{ij} = \frac{i}{2}(\gamma^i\gamma^j - \gamma^j\gamma^i) \tag{6}$$

$$\omega_{\mu ij} = g^E_{\alpha\beta} e^\alpha_i (\partial_\mu e^\beta_j + \Gamma^\beta_{\nu\mu} e^\nu_j) \tag{7}$$

where e^μ_i is the vierbein and $\Gamma^\alpha_{\mu\nu}$ is the Christoffel symbol.

[2] A. Yamamoto and Y. Hirono, Phys. Rev. Lett. **111**, 081601 (2013), arXiv:1303.6292 [hep-lat].

Rotating QCD: sign problem

The Euclidean metric tensor can be obtained from $g_{\mu\nu}$ by Wick rotation $t \to i\tau$

$$g^E_{\mu\nu} = \begin{pmatrix} 1 & 0 & 0 & y\Omega_I \\ 0 & 1 & 0 & -x\Omega_I \\ 0 & 0 & 1 & 0 \\ y\Omega_I & -x\Omega_I & 0 & 1 + r^2\Omega_I^2 \end{pmatrix},$$

where imaginary angular velocity $\Omega_I = -i\Omega$ is introduced.

Rotating QCD: sign problem

The Euclidean metric tensor can be obtained from $g_{\mu\nu}$ by Wick rotation $t \to i\tau$

$$g^E_{\mu\nu} = \begin{pmatrix} 1 & 0 & 0 & y\Omega_I \\ 0 & 1 & 0 & -x\Omega_I \\ 0 & 0 & 1 & 0 \\ y\Omega_I & -x\Omega_I & 0 & 1 + r^2\Omega_I^2 \end{pmatrix},$$

where imaginary angular velocity $\Omega_I = -i\Omega$ is introduced.

Sign problem

- The Euclidean action is complex-valued function with real rotation!
- The Monte–Carlo simulations are conducted with imaginary angular velocity
- The results are analytically continued to the region of the real angular velocity.

Lattice setup

The resulting partition function is

$$Z = \int D\psi\, D\bar{\psi}\, DU\, \exp\big(- S_G[U, \Omega_I] - S_F[\bar{\psi}, \psi, m, U, \Omega_I]\big) = \\ = \int DU\, \det M[m, U, \Omega_I]\, e^{(-S_G[U,\Omega_I])} \quad (8)$$

- $N_f = 2$ clover-improved Wilson fermions (c_{SW} from one-loop) + RG-improved (Iwasaki) gauge action are used.
- We reanalyze data for $m_{PS}a$ and $m_V a$ at zero temperature from CP-PACS and WHOT-QCD collaborations to restore LCP's more frequently in β and set the scale.
- Simulation is performed on the lattice $N_t \times N_z \times N_s^2$ $(N_s = N_x = N_y)$, which rotates around z-axis.
  Up to now, only results with $N_t = 4$ are available, work in progress...

LCP and scale setting

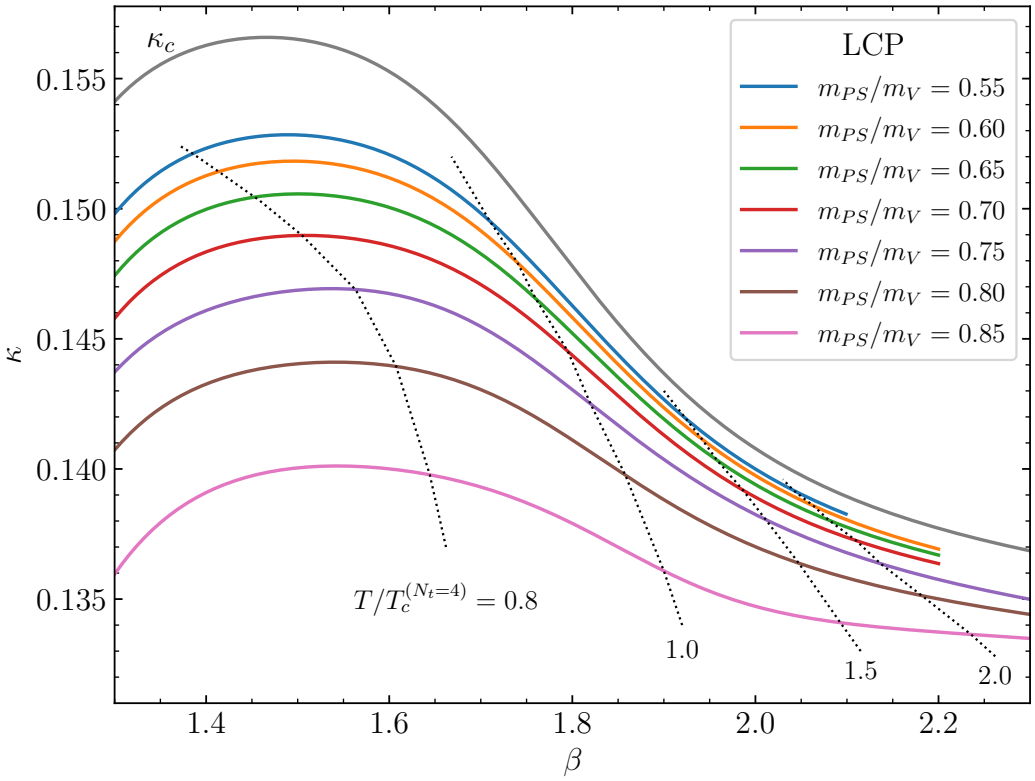

To set the temperature along the given LCP we use the zero-temperature mass of vector meson (m_V-input)

$$\frac{T}{m_V}(m_{PS}/m_V, \beta) = \frac{1}{N_t \times m_V a(m_{PS}/m_V, \beta)} \,. \tag{9}$$

and find

$$\frac{T}{T_{pc}}(\beta) = \frac{m_V a(\beta_{pc,\Omega=0})}{m_V a(\beta)}$$

Lattice setup: rotation and boundary conditions

- The system should be limited in the directions, which are orthogonal to the rotation axis: $\Omega(N_s - 1)a/\sqrt{2} < 1$

Lattice setup: rotation and boundary conditions

- The system should be limited in the directions, which are orthogonal to the rotation axis: $\Omega(N_s - 1)a/\sqrt{2} < 1$

$$\Downarrow$$

- The use of periodic/open/Dirichlet BC gives qualitatively the same results for rotating gluodynamics (boundary is screened). PBC in directions x, y are used.
- The critical temperature in gluodynamics depends mainly on the linear velocity on the boundary $v_I = \Omega_I(N_s - 1)a$. Thus, v_I is fixed in simulations instead of angular velocity Ω_I in physical units (e.g., MeV).

Observables

- The Polyakov loop is

$$L(\vec{x}) = \mathrm{Tr}\left[\prod_{\tau=0}^{N_t-1} U_4(\vec{x},\tau)\right], \qquad L = \frac{1}{N_s^2 N_z}\sum_{\vec{x}} L(\vec{x})\,. \tag{10}$$

The pseudo-critical temperature T_{pc} of the confinement/deconfinement transition is determined using the Polyakov loop susceptibility

$$\chi_L = N_s^2 N_z \left(\langle |L|^2\rangle - \langle |L|\rangle^2\right), \tag{11}$$

by means of the Gaussian fit.

- The (bare) chiral condensate is

$$\langle\bar{\psi}\psi\rangle^{bare} = -\frac{N_f T}{V}\left\langle \mathrm{Tr}(M^{-1})\right\rangle \tag{12}$$

For the chiral transition, pseudo-critical temperature T_{pc} is determined using peak of the (disconnected) chiral susceptibility:

$$\chi^{bare}_{\langle\bar{\psi}\psi\rangle} = \frac{N_f T}{V}\left[\left\langle \mathrm{Tr}(M^{-1})^2\right\rangle - \left\langle \mathrm{Tr}(M^{-1})\right\rangle^2\right] \tag{13}$$

Rotating QCD: Periodic boundary conditions

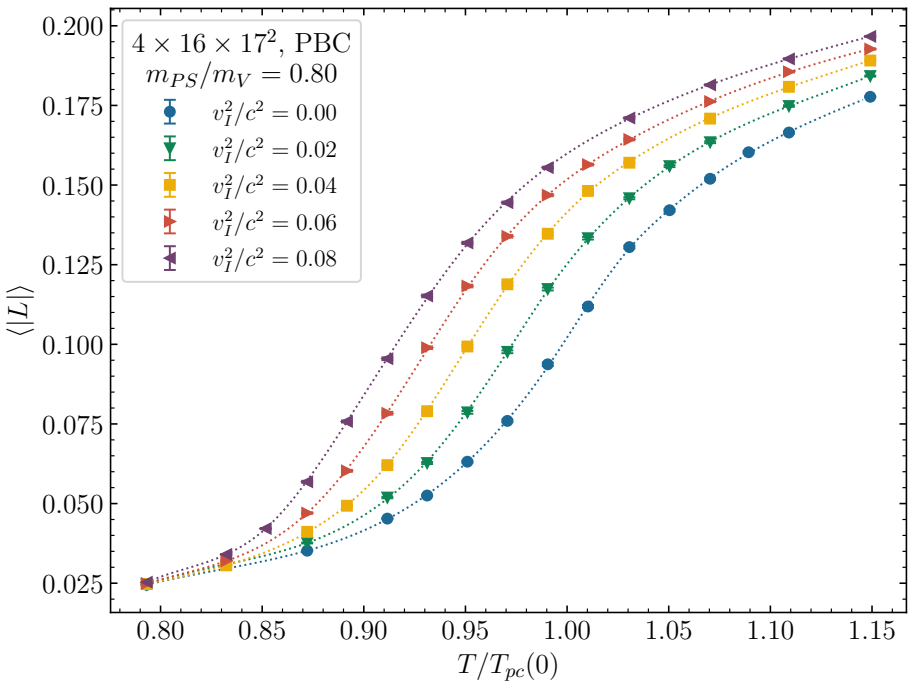

Figure: The Polyakov loop as a function of $T/T_{pc}(\Omega = 0)$ for different values of imaginary linear velocity on the boundary v_I. Lattice $4 \times 16 \times 17^2$, LCP $m_{PS}/m_V = 0.80$.

- Pseudo-critical temperature decreases due to imaginary rotation (like in gluodynamics).

Rotating QCD: Periodic boundary conditions

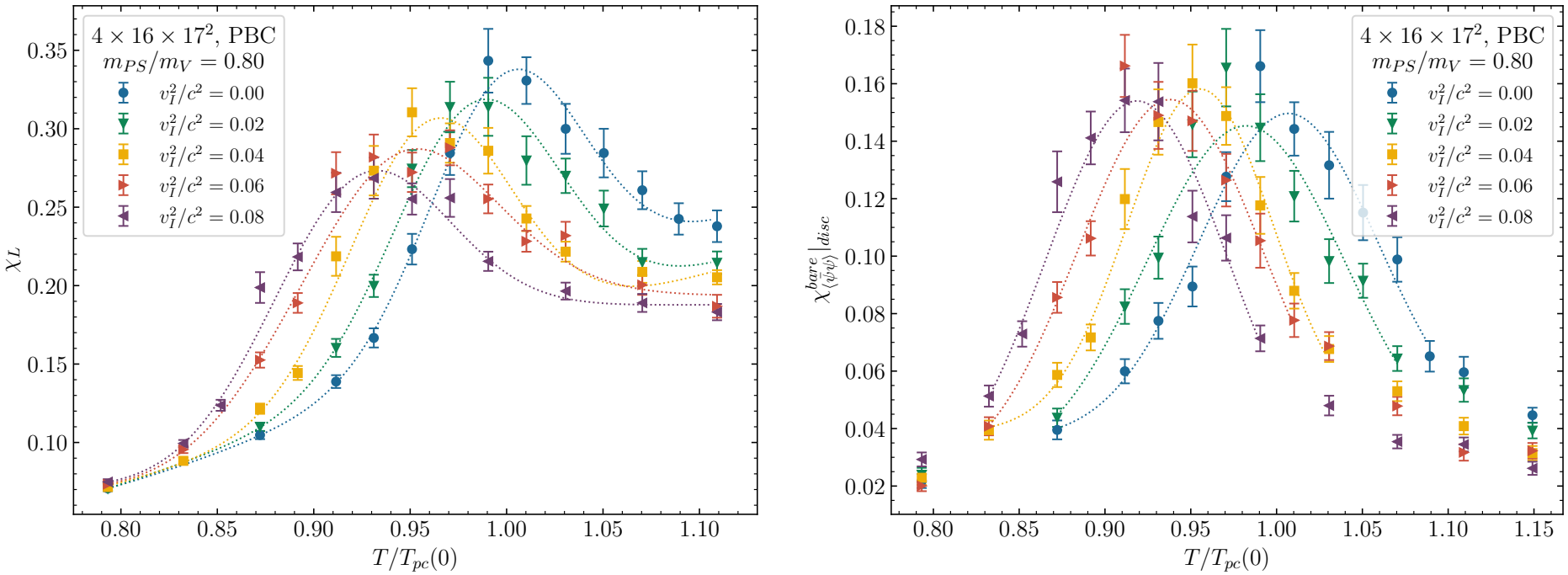

Figure: The Polyakov loop susceptibility and chiral susceptibility as a function of $T/T_{pc}(\Omega = 0)$ for different values of imaginary linear velocity on the boundary v_I. Lattice $4 \times 16 \times 17^2$, LCP $m_{PS}/m_V = 0.80$.

- Pseudo-critical temperature decreases due to imaginary rotation (like in gluodynamics).

Rotating QCD: Periodic boundary conditions

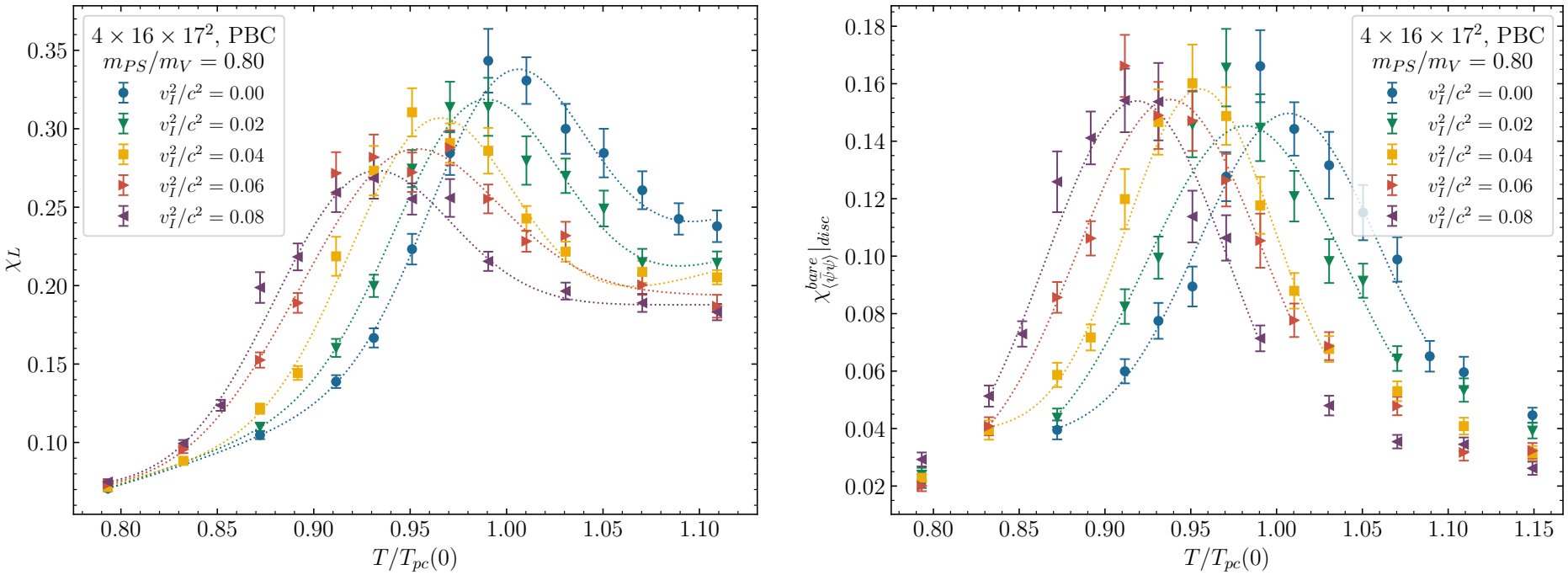

Figure: The Polyakov loop susceptibility and chiral susceptibility as a function of $T/T_{pc}(\Omega = 0)$ for different values of imaginary linear velocity on the boundary v_I. Lattice $4 \times 16 \times 17^2$, LCP $m_{PS}/m_V = 0.80$.

- Pseudo-critical temperature decreases due to imaginary rotation (like in gluodynamics).

In order to disentangle the effect of the rotation on fermions and gluons, the separate angular velocities are introduced: $S_G(\Omega_G) + S_F(\Omega_F)$.

Rotating QCD: various rotation regimes

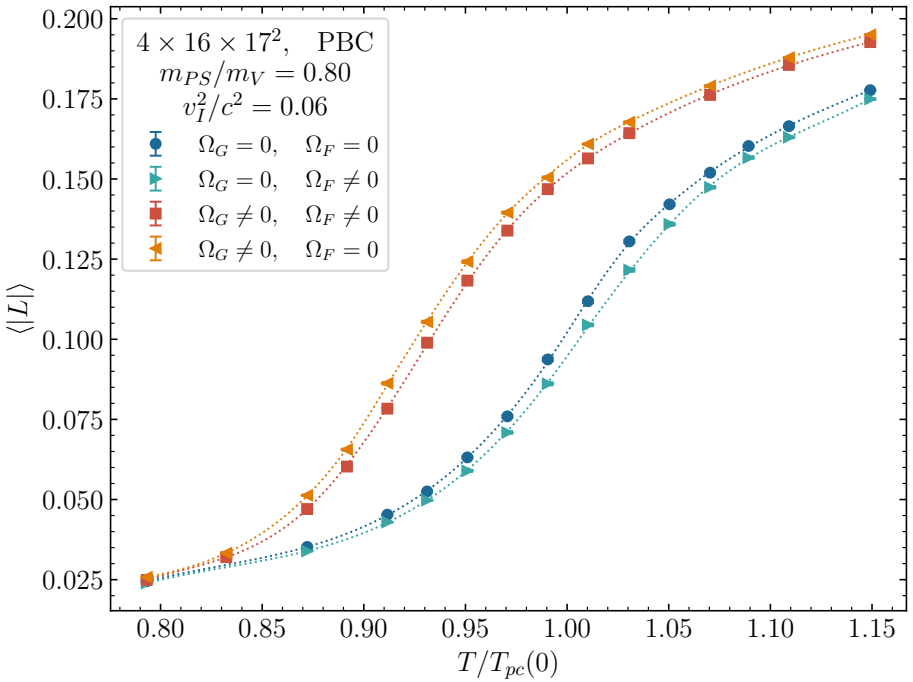

Figure: The Polyakov loop as a function of T/T_{pc} for various rotation regimes. Lattice $4 \times 16 \times 17^2$, $m_{PS}/m_V = 0.80$.

Rotating QCD: various rotation regimes

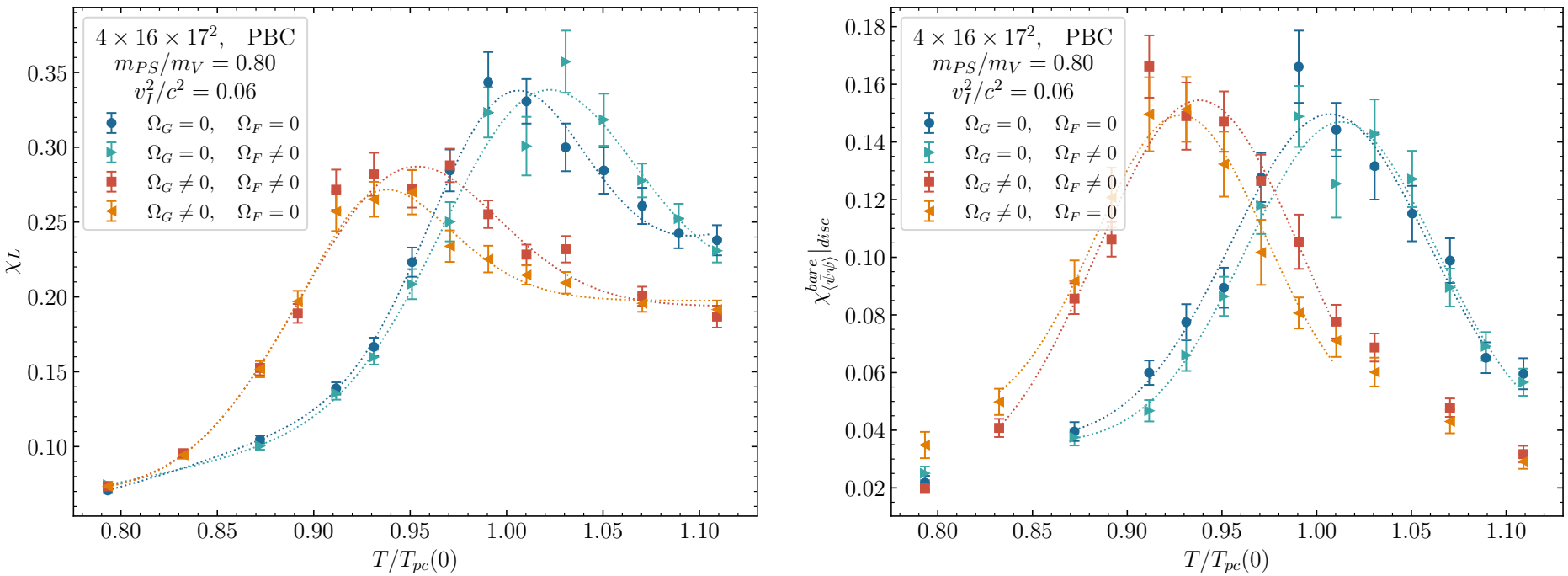

Figure: The Polyakov loop susceptibility and chiral susceptibility as a function of T/T_{pc} for various rotation regimes. Lattice $4 \times 16 \times 17^2$, $m_{PS}/m_V = 0.80$.

- Rotation of fermions and gluons separately has the opposite influence on the critical temperature.

Rotating QCD: various rotation regimes

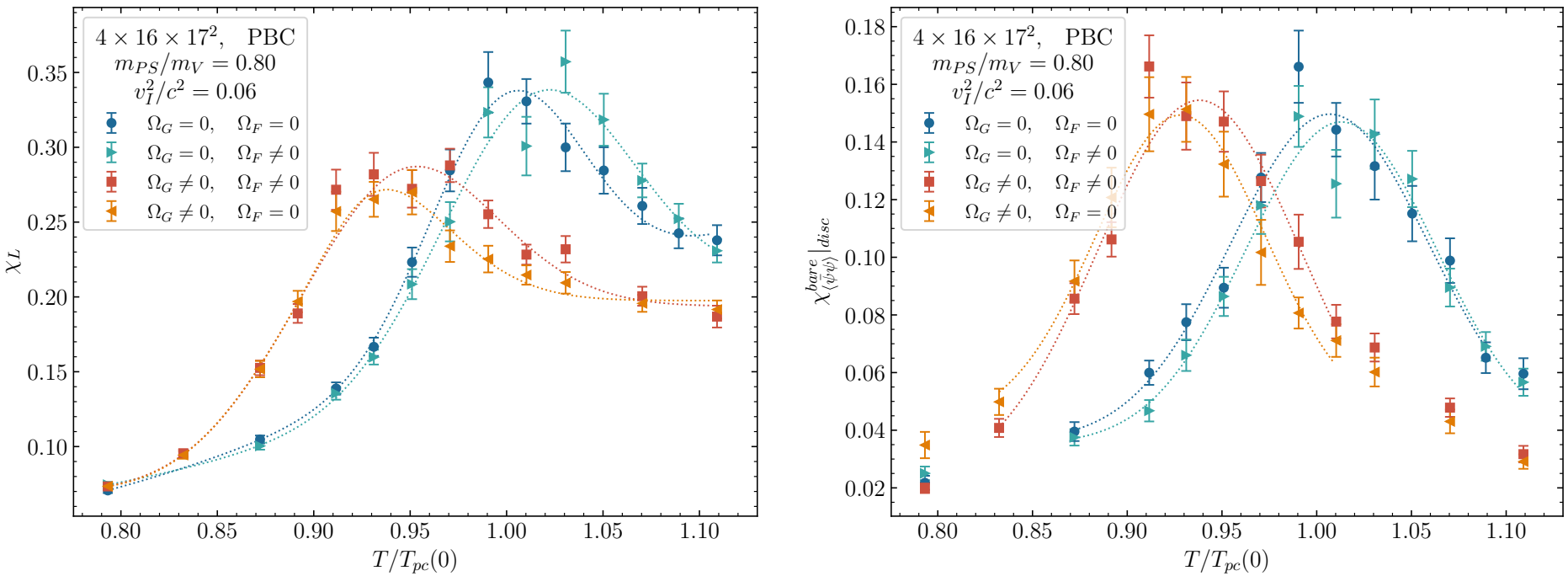

Figure: The Polyakov loop susceptibility and chiral susceptibility as a function of T/T_{pc} for various rotation regimes. Lattice $4 \times 16 \times 17^2$, $m_{PS}/m_V = 0.80$.

- Rotation of fermions and gluons separately has the opposite influence on the critical temperature.
- But only the regime $\Omega_G = \Omega_F$ is physical.

Rotating QCD: critical temperature

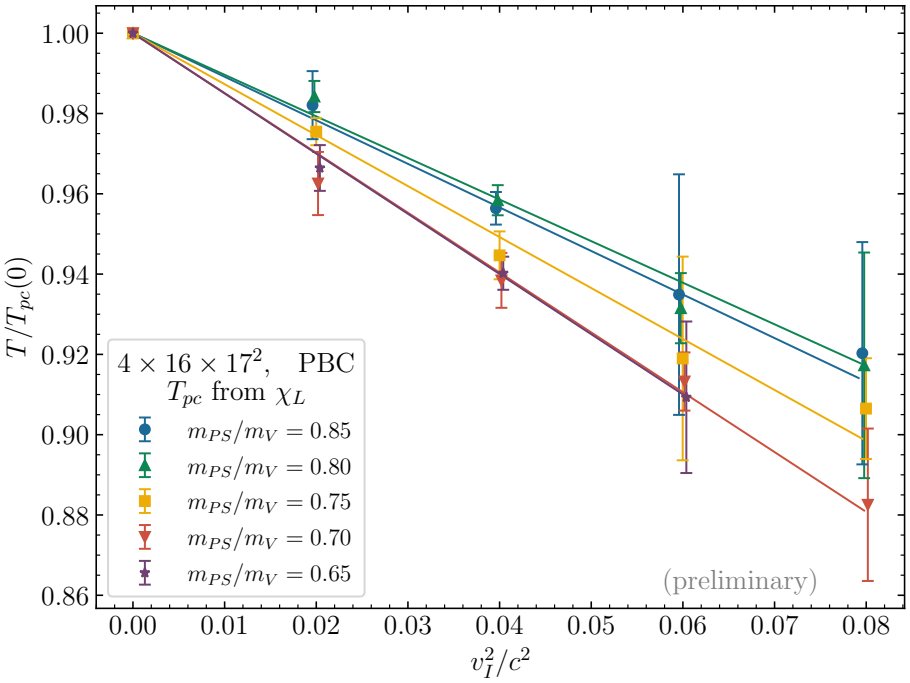

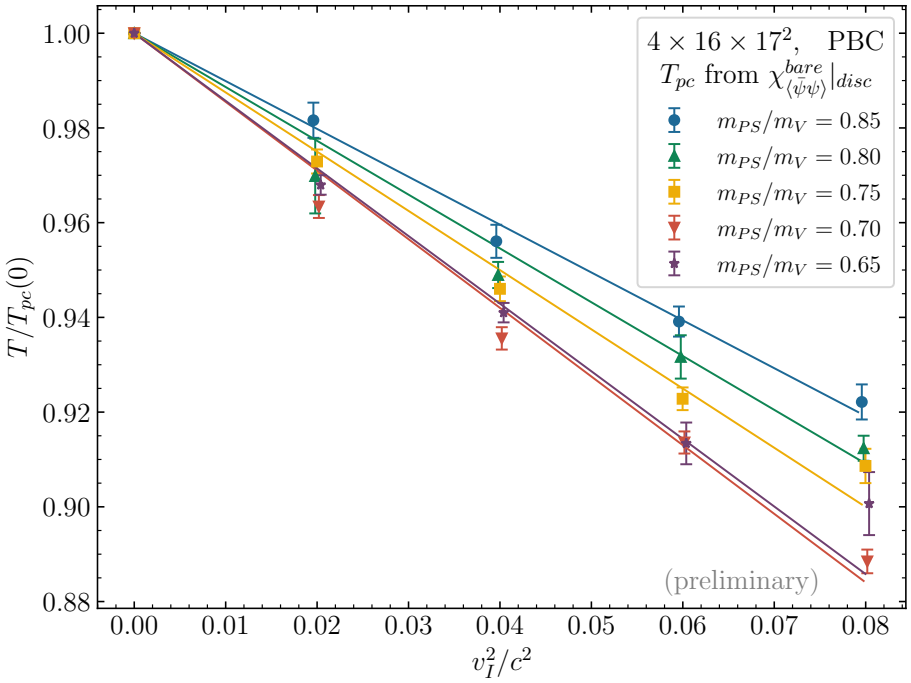

LCP's with $m_{PS}/m_V = 0.65, 0.70, 0.75, 0.80, 0.85$ were considered; $v_I/c < 0.3$.

$$\frac{T_{pc}(v_I)}{T_{pc}(0)} = 1 - B_2 \frac{v_I^2}{c^2}$$

Rotating QCD: critical temperature

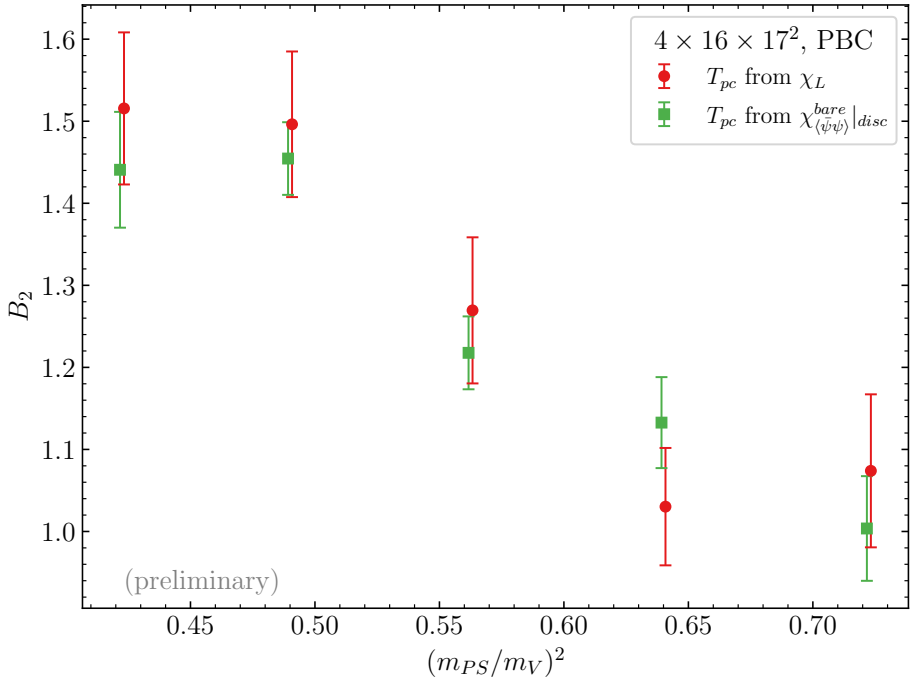

LCP's with $m_{PS}/m_V = 0.65, 0.70, 0.75, 0.80, 0.85$ were considered; $v_I/c < 0.3$.

$$\frac{T_{pc}(v_I)}{T_{pc}(0)} = 1 - B_2 \frac{v_I^2}{c^2} \qquad \Longrightarrow \qquad \frac{T_{pc}(v)}{T_{pc}(0)} = 1 + B_2 \frac{v^2}{c^2}$$

- The pseudo-critical temperature increases with the angular velocity ($v \propto \Omega$).
- The coefficient B_2 slightly grows with approaching to chiral limit.
- The chiral transition shifts to the same direction as confinement-deconfinement transition.

Conclusions

- The separate rotation of quarks and gluons in QCD has the opposite influence on the critical temperature.
- The critical temperature in $N_f = 2$ QCD increases with angular velocity ($v \propto \Omega$)

$$\frac{T_{pc}(v)}{T_{pc}(0)} = 1 + B_2 \frac{v^2}{c^2} \, .$$

  It's not Tolman-Ehrenfest effect!
- The coefficient B_2 slightly grows with decreasing pion mass in considered range ($m_{PS}/m_V = 0.65 \ \ldots \ 0.85$).
- The (preliminary) results are similar to gluodynamics, where the critical temperature also increases with angular velocity.
- It should be noted, that NJL (and other phenomenological models) predicts that critical temperature decreases due to the rotation. But taking into account the contribution of rotating gluons leads to an increase in T_c.

- Future plans: increase statistics; simulations with smaller pion mass, on finer lattices ($N_t = 6, 8$), with an open BC.

Thank you for your attention!

Rotating QCD: various rotation regimes

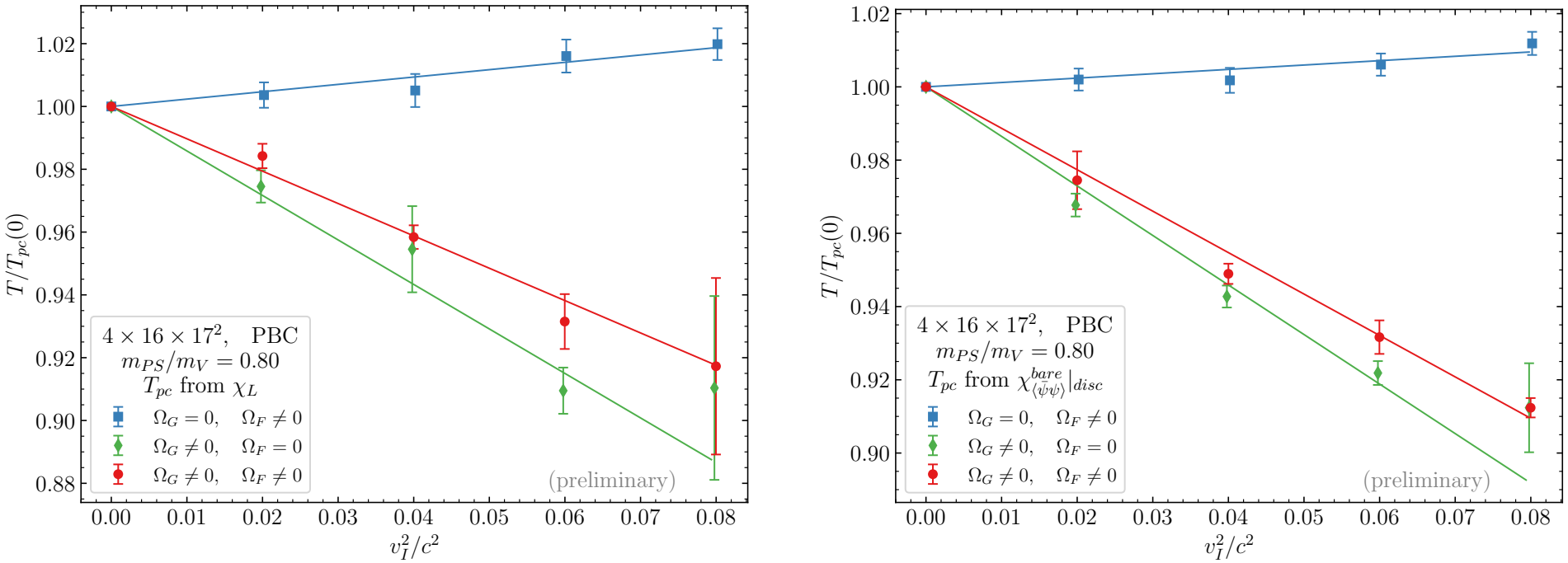

Figure: The pseudo-critical temperature as a function of imaginary linear velocity on the boundary for various rotation regimes (full, only gluons, only fermions).

$$\frac{T_{pc}(v_I)}{T_{pc}(0)} = 1 - B_2 \frac{v_I^2}{c^2} \tag{14}$$

$\Omega_G = \Omega_F \neq 0$	$\Omega_G \neq 0$	$\Omega_F \neq 0$
$B_2 > 0$	$B_2^{(G)} > B_2$	$B_2^{(F)} < 0$

Rotating reference frame: temperature

$$\int d^4x\sqrt{g_E}\,(\dots) = \int_0^{1/T} dx_0\sqrt{g_{44}}\int d^3x\sqrt{\gamma_E}\,(\dots) = \int_0^{1/T} dx_0\int d^3x\sqrt{g_E}\,(\dots)$$

- Interpretation: Tolman-Ehrenfest effect. In gravitational field the temperature isn't a constant in space at thermal equilibrium:

$$T(r)\sqrt{g_{00}} = const\,,$$

Rotating reference frame: temperature

$$\int d^4x\sqrt{g_E}\,(\dots) = \int_0^{1/T} dx_0\sqrt{g_{44}}\int d^3x\sqrt{\gamma_E}\,(\dots) = \int_0^{1/T} dx_0\int d^3x\sqrt{g_E}\,(\dots)$$

- Interpretation: Tolman-Ehrenfest effect. In gravitational field the temperature isn't a constant in space at thermal equilibrium:

$$T(r)\sqrt{g_{00}} = const\,,$$

- For the (real) rotation one has

$$T(r)\sqrt{1-r^2\Omega^2} = const \equiv T\,,$$

- One could expect, that the rotation effectively warm up the periphery of the modeling volume

$$T(r) > T(r=0),$$

and as a result, from kinematics, the critical temperature should decreases.

Rotating QCD: continuum gluon action

The Euclidean metric tensor can be obtained from $g_{\mu\nu}$ by Wick rotation $t \to i\tau$

$$g^E_{\mu\nu} = \begin{pmatrix} 1 & 0 & 0 & y\Omega_I \\ 0 & 1 & 0 & -x\Omega_I \\ 0 & 0 & 1 & 0 \\ y\Omega_I & -x\Omega_I & 0 & 1 + r^2\Omega_I^2 \end{pmatrix},$$

where imaginary angular velocity $\Omega_I = -i\Omega$ is introduced. Substituting the $(g_E)_{\mu\nu}$ to formula (15) one gets

$$S_G = \frac{1}{2g^2}\int d^4x \Big[(1 + r^2\Omega_I^2)F^a_{xy}F^a_{xy} + (1 + y^2\Omega_I^2)F^a_{xz}F^a_{xz} + (1 + x^2\Omega_I^2)F^a_{yz}F^a_{yz} +$$
$$+ F^a_{x\tau}F^a_{x\tau} + F^a_{y\tau}F^a_{y\tau} + F^a_{z\tau}F^a_{z\tau} -$$
$$+ 2y\Omega_I(F^a_{xy}F^a_{y\tau} + F^a_{xz}F^a_{z\tau}) - 2x\Omega_I(F^a_{yx}F^a_{x\tau} + F^a_{yz}F^a_{z\tau}) + 2xy\Omega_I^2F^a_{xz}F^a_{zy}\Big].$$

Rotating QCD: continuum quark action

The covariant Dirac operator depends on the choice of the vierbein. We choose the vierbein in the form[3]

$$e_1^x = e_2^y = e_3^z = e_4^\tau = 1\,, \quad e_4^x = -y\Omega_I\,, \quad e_4^y = x\Omega_I\,, \quad \text{and other } e_i^\mu = 0$$

As the result, the Euclidean quark action is

$$S_F = \int d^4x\,\bar{\psi}\left(\gamma^x D_x + \gamma^y D_y + \gamma^z D_z + \gamma^\tau\left(D_\tau + i\Omega_I\frac{\sigma^{12}}{2}\right) + m\right)\psi\,, \tag{15}$$

where the gamma matrices are given by $\gamma^\mu = \gamma^i e_i^\mu$

$$\gamma^x = \gamma^1 - y\Omega_I\gamma^4\,, \quad \gamma^y = \gamma^2 + x\Omega_I\gamma^4\,, \quad \gamma^z = \gamma^3\,, \quad \gamma^\tau = \gamma^4\,. \tag{16}$$

The quark action contains orbit-rotation coupling term $\gamma^\tau\Omega_I(xD_y - yD_x)$ and spin-rotation coupling term $i\gamma^\tau\Omega_I\sigma^{12}/2$.

[3] A. Yamamoto and Y. Hirono, Phys. Rev. Lett. **111**, 081601 (2013), arXiv:1303.6292 [hep-lat].

Rotating QCD: gluon lattice action

We use RG-improved (Iwasaki) lattice gauge action (for non-rotating part):

$$S_G = \beta \sum_x \Big((c_0 + r^2\Omega_I^2) W_{xy}^{1\times1} + (c_0 + y^2\Omega_I^2) W_{xz}^{1\times1} + (c_0 + x^2\Omega_I^2) W_{yz}^{1\times1} + \\ + c_0 \big(W_{x\tau}^{1\times1} + W_{y\tau}^{1\times1} + W_{z\tau}^{1\times1} \big) + y\Omega_I \big(W_{xy\tau}^{1\times1\times1} + W_{xz\tau}^{1\times1\times1} \big) - \\ - x\Omega_I \big(W_{yx\tau}^{1\times1\times1} + W_{yz\tau}^{1\times1\times1} \big) + xy\Omega_I^2 W_{xzy}^{1\times1\times1} + \sum_{\mu\neq\nu} c_1 W_{\mu\nu}^{1\times2} \Big) , \quad (17)$$

with $\beta = 6/g^2$, and $c_0 = 1 - 8c_1$, and $c_1 = -0.331$, where

$$W_{\mu\nu}^{1\times1}(x) = 1 - \frac{1}{3}\mathrm{Re\ Tr}\ \bar{U}_{\mu\nu}(x) , \quad (18)$$

$$W_{\mu\nu}^{1\times2}(x) = 1 - \frac{1}{3}\mathrm{Re\ Tr}\ R_{\mu\nu}(x) , \quad (19)$$

$$W_{\mu\nu\rho}^{1\times1\times1}(x) = -\frac{1}{3}\mathrm{Re\ Tr}\ \bar{V}_{\mu\nu\rho}(x) , \quad (20)$$

$\bar{U}_{\mu\nu}$ denotes clover-type average of 4 plaquettes,

$R_{\mu\nu}$ is a rectangular loop,

$\bar{V}_{\mu\nu\rho}$ is asymmetric chair-type average of 8 chairs.

Rotating QCD: quark lattice action

The lattice quark action has the following form ($N_f = 2$ clover-improved Wilson fermions are used)

$$S_F = \sum_f \sum_{x_1,x_2} \bar{\psi}^f(x_1) \Bigg\{ \delta_{x_1,x_2} - \kappa \Bigg[(1-\gamma^x)T_{x+} + (1+\gamma^x)T_{x-} + (1-\gamma^y)T_{y+} + (1+\gamma^y)T_{y-} + (1-\gamma^z)T_{z+} + (1+\gamma^z)T_{z-} + (1-\gamma^\tau)\exp\left(ia\Omega_I \frac{\sigma^{12}}{2}\right)T_{\tau+} + (1+\gamma^\tau)\exp\left(-ia\Omega_I \frac{\sigma^{12}}{2}\right)T_{\tau-} \Bigg] - \delta_{x_1,x_2} c_{SW}\kappa \sum_{\mu<\nu} \sigma_{\mu\nu}F_{\mu\nu} \Bigg\} \psi^f(x_2), \quad (21)$$

where $\kappa = 1/(8+2am)$, $\quad T_{\mu+} = U_\mu(x_1)\delta_{x_1+\mu,x_2}$, $\quad T_{\mu-} = U^\dagger_\mu(x_1)\delta_{x_1-\mu,x_2}$ and

$$\gamma^x = \gamma^1 - y\Omega_I\gamma^4, \quad \gamma^y = \gamma^2 + x\Omega_I\gamma^4, \quad \gamma^z = \gamma^3, \quad \gamma^\tau = \gamma^4.$$

The clover coefficient is taken as $c_{SW} = (1 - W^{1\times1})^{-3/4} = (1 - 0.8412/\beta)^{-3/4}$ (one-loop result for the plaquette are used).

The spin-rotation coupling term is exponentiated like chemical potential.

Rotating QCD: quark lattice action

The lattice quark action has the following form ($N_f = 2$ clover-improved Wilson fermions are used)

$$S_F = \sum_f \sum_{x_1,x_2} \bar{\psi}^f(x_1) \Bigg\{ \delta_{x_1,x_2} - \kappa \Bigg[(1-\gamma^x) T_{x+} + (1+\gamma^x) T_{x-} + (1-\gamma^y) T_{y+} + (1+\gamma^y) T_{y-} + (1-\gamma^z) T_{z+} + (1+\gamma^z) T_{z-} + (1-\gamma^\tau) \exp\left(ia\Omega_I \frac{\sigma^{12}}{2} \right) T_{\tau+} + (1+\gamma^\tau) \exp\left(-ia\Omega_I \frac{\sigma^{12}}{2} \right) T_{\tau-} \Bigg] - \delta_{x_1,x_2} c_{SW} \kappa \sum_{\mu<\nu} \sigma_{\mu\nu} F_{\mu\nu} \Bigg\} \psi^f(x_2), \quad (21)$$

where $\kappa = 1/(8+2am)$, $\quad T_{\mu+} = U_\mu(x_1)\delta_{x_1+\mu,x_2}$, $\quad T_{\mu-} = U^\dagger_\mu(x_1)\delta_{x_1-\mu,x_2}$ and

$$\gamma^x = \gamma^1 - y\Omega_I\gamma^4, \quad \gamma^y = \gamma^2 + x\Omega_I\gamma^4, \quad \gamma^z = \gamma^3, \quad \gamma^\tau = \gamma^4.$$

The clover coefficient is taken as $c_{SW} = (1 - W^{1\times1})^{-3/4} = (1 - 0.8412/\beta)^{-3/4}$ (one-loop result for the plaquette are used).

The spin-rotation coupling term is exponentiated like chemical potential.

Rotating gluodynamics: OBC, Polyakov loop distribution

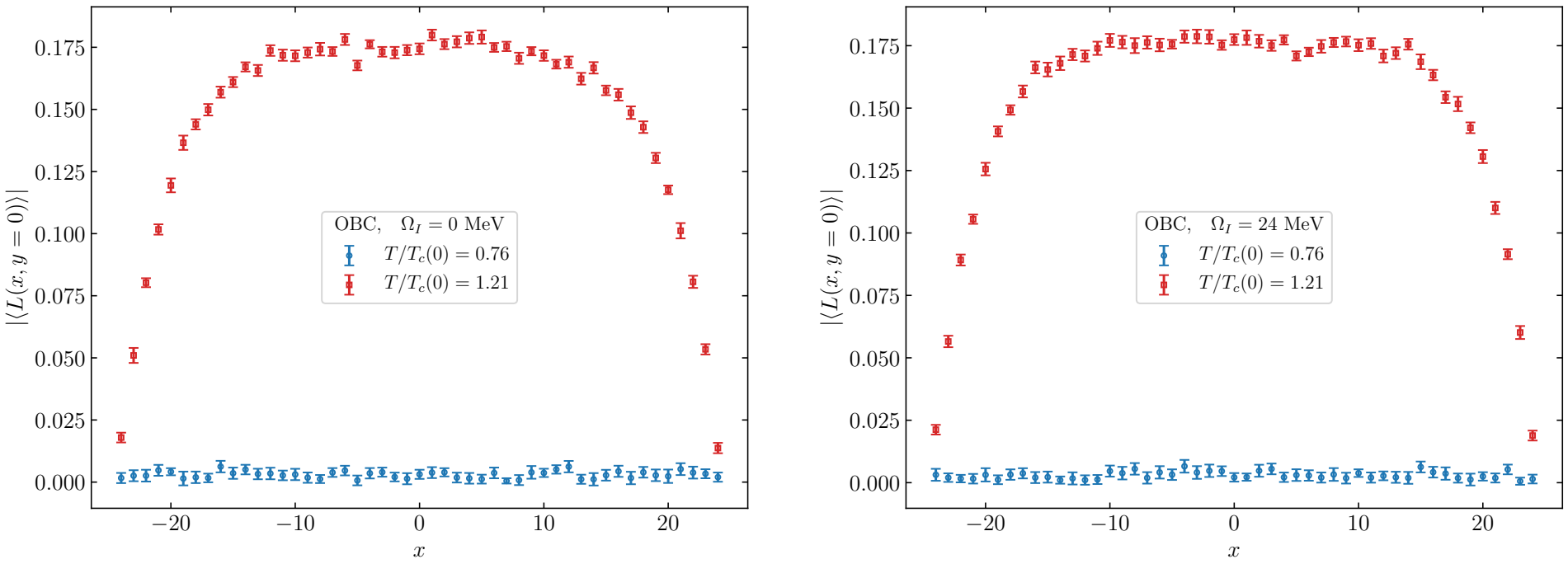

Figure: The local Polyakov loop $|\langle L(x, y)\rangle|$ as a function of coordinate for OBC and $\Omega_I = 0$ MeV (left), $\Omega_I = 24$ MeV (right). Points with $x \neq 0, y = 0$ from the lattice $8 \times 24 \times 49^2$ are shown.

- The local Polyakov loop $|\langle L(x, y)\rangle|$ is zero for all spatial points in the confinement phase, both with and without rotation $\Rightarrow$ Polyakov loop still acts as the order parameter.
- In deconfinement phase the boundary is screened.

Rotating gluodynamics: PBC, Polyakov loop distribution

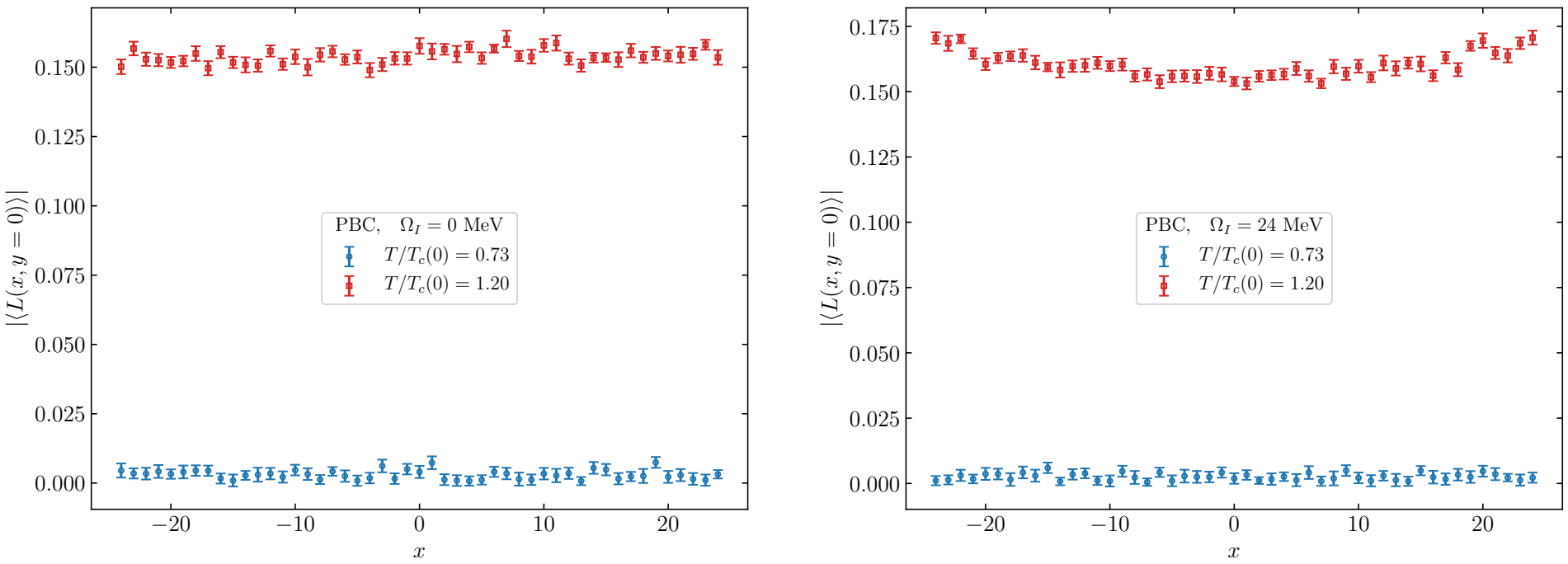

Figure: The local Polyakov loop $|\langle L(x, y)\rangle|$ as a function of coordinate for OBC and $\Omega_I = 0$ MeV (left), $\Omega_I = 24$ MeV (right). Points with $x \neq 0, y = 0$ from the lattice $8 \times 24 \times 49^2$ are shown.

- The local Polyakov loop $|\langle L(x, y)\rangle|$ is zero for all spatial points in the confinement phase, both without rotation and with nonzero angular velocity.
- The local Polyakov loop demonstrates weak dependence on the coordinate in the deconfinement phase.

Rotating gluodynamics: DBC, Polyakov loop distribution

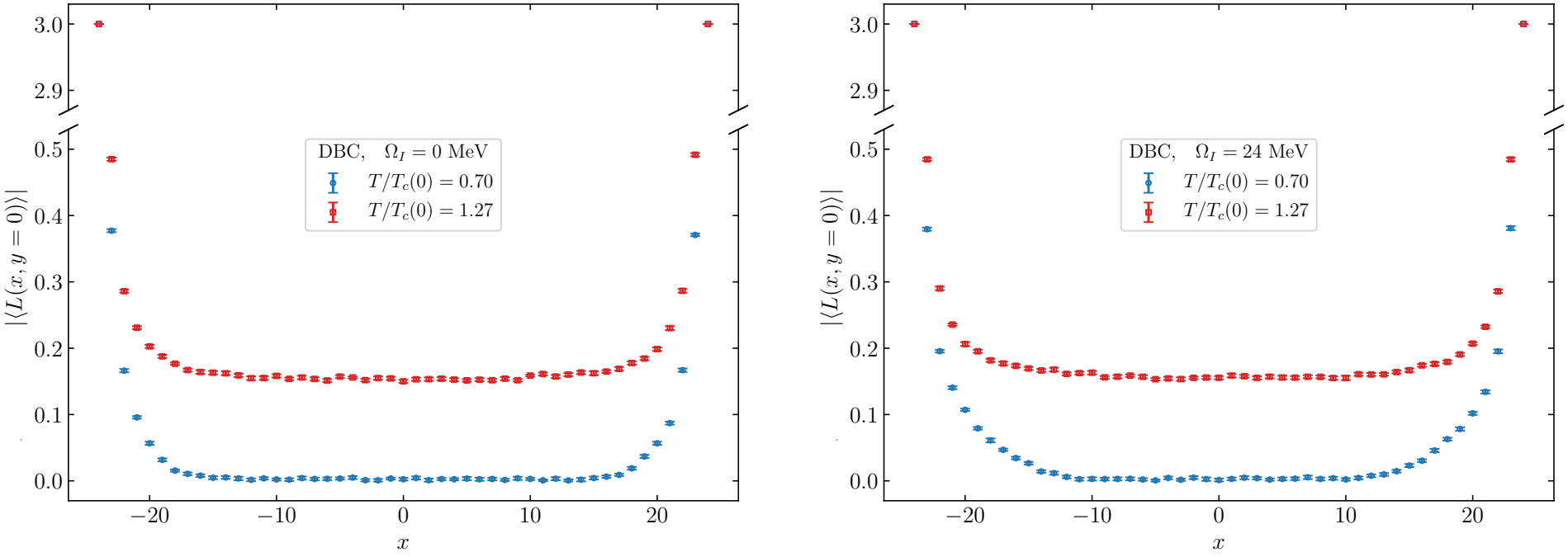

Figure: The local Polyakov loop $|\langle L(x, y)\rangle|$ as a function of coordinate for OBC and $\Omega_I = 0$ MeV (left), $\Omega_I = 24$ MeV (right). Points with $x \neq 0, y = 0$ from the lattice $8 \times 24 \times 49^2$ are shown.

- The local Polyakov loop $|\langle L(x, y)\rangle|$ is equal three on the boundary in both phases.
- The boundary is screened.